Tunable Visible and Near Infrared Photoswitches

James R. Hemmer,[†] Saemi O. Poelma,[†] Nicolas Treat,[‡] Zachariah A. Page,[‡] Neil D. Dolinski,[‡] Yvonne J. Diaz,[†] Warren Tomlinson,[§] Kyle D. Clark,[†] Joseph P. Hooper,[§] Craig Hawker,[‡,†] and Javier Read de Alaniz*[,†]

[†]Department of Chemistry and Biochemistry and [‡]Materials Department, Materials Research Laboratory, University of California, Santa Barbara, California 93106, United States

[§]Department of Physics, Naval Postgraduate School, 1 University Circle, Monterey, California 93943, United States

S Supporting Information

ABSTRACT: A class of tunable visible and near-infrared donor−acceptor Stenhouse adduct (DASA) photoswitches were efficiently synthesized in two to four steps from commercially available starting materials with minimal purification. Using either Meldrum's or barbituric acid "acceptors" in combination with aniline-based "donors", an absorption range spanning from 450 to 750 nm is obtained. Additionally, photoisomerization results in complete decoloration for all adducts, yielding fully transparent, colorless solutions and films. Detailed investigations using density functional theory, nuclear magnetic resonance, and visible absorption spectroscopies provide valuable insight into the unique structure−property relationships for this novel class of photoswitches. As a final demonstration, selective photochromism is accomplished in a variety of solvents and polymer matrices, a significant advantage for applications of this new generation of DASAs.
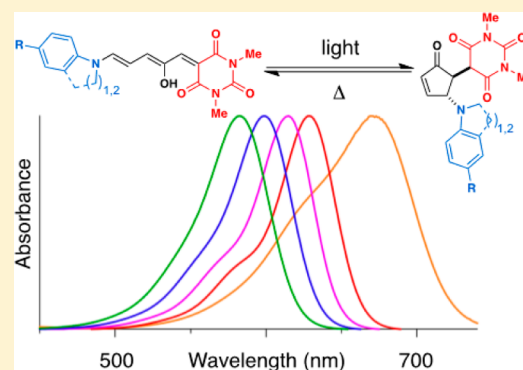
INTRODUCTION

Photoswitches have long held the interest of the scientific community for their ability to alter molecular structure, and thus properties, using light as a stimulus.[1−3] Upon photoexcitation, the photoswitch transforms from a thermodynamically stable state to a metastable photostationary state. In the photostationary state, molecules will return to equilibrium by thermal relaxation or upon photoirradiation with a different wavelength. The resulting change in structure can modify absorption, polarity, and/or free volume. Not surprisingly, numerous applications have taken advantage of these property changes including switching of surface polarity,[4] membrane permeability,[5] nanoparticle clustering,[6,7] as well as controlling the properties of biologically active molecules.[8−12] Additionally, photoswitches have been used to create mechanical actuators[13] and mechanical sensors[14] (mechanophores).

Although photoswitches have been extensively studied for over a century, the most widely used classes, including azobenzene,[15] diarylethene,[16] dihydroazulene,[17] and spiropyran,[18] often reside in a colorless thermodynamically stable state that requires high-energy ultraviolet (UV) light for activation. The use of UV light comes with inherent limitations for a range of applications that arise from irreversible chemical damage and limited penetration depth in many materials. Alternatively, low-energy visible light-activated photoswitches, described as negative photochromes owing to their colored thermodynamically stable state, have the potential to overcome such limitations yet are far less common.[19−23]

In the past decade, advances with azobenzene-based photoswitches demonstrated by Aprahamian,[24,25] Hecht,[26] Herges,[27] and Woolley[8] have allowed for visible light isomerization across a broad range of wavelengths. However, in these photochromic systems, switching occurs between two colored states. This feature limits their use in applications such as sensing that benefit from a more notable color change.[28] Although conversion from colorless-to-colored is routine for spiropyran derivatives, they have been shown to fatigue quickly upon repeated cycling experiments. Exposure to high-energy UV light and the presence of singlet and triplet oxygen have been identified as key factors leading to degradation.[29,30] To address these challenges, we sought to design a robust and highly tunable photoswitch platform using inexpensive reagents and simple syntheses to provide a colored-to-colorless transformation using visible light.

Donor−acceptor Stenhouse adducts (DASAs) are a new class of negative photoswitches that can be synthesized easily in two steps from commercially available starting materials.[31] The colored DASA becomes colorless upon irradiation with visible light. This process initiates with a light-controlled alkene isomerization followed by a thermal 4π electrocyclization to the colorless state. In initial work, we described DASAs containing alkyl-based amine "donors" (electron-rich) and Meldrum's or barbituric acid "acceptors" (electron-deficient) that display

visible light absorption, high fatigue resistance, and a significant polarity and color change upon switching.[32] However, with these first-generation DASAs, wavelength tunability was limited to 545 and 570 nm for the Meldrum's and barbituric acid derivatives, respectively.[31] Additionally, reversible photoswitching was only possible in nonpolar solvents such as toluene, and reversible switching could not be observed in solid-supported matrices.[33,34] To improve the performance of DASA-based photoswitches, we have designed a new system that overcomes these limitations while retaining the facile two-step synthetic approach from commercially available materials. Specifically, we report a study using secondary aniline-derivatives as donors to provide wavelength tunable DASA photochromes (Figure 1)
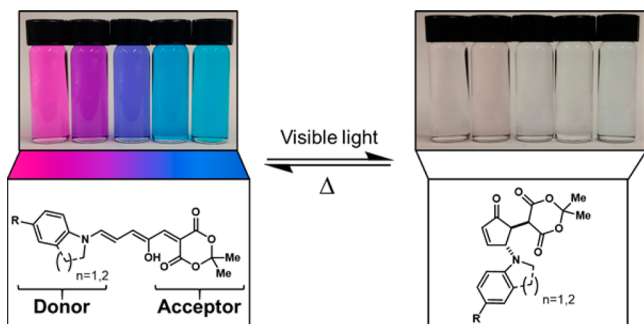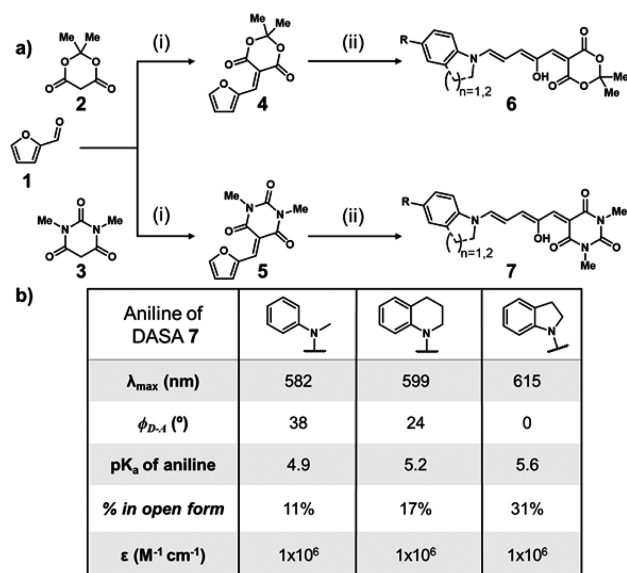

Figure 1. General structure for second generation donor−acceptor Stenhouse adducts containing aniline-based donors and a Meldrum's acid acceptor. The thermodynamically stable colored "open" isomer (left) can be converted into the photostationary colorless "closed" isomer (right) with visible light irradiation.

Figure 2. Synthesis and characterization of aniline-based donor−acceptor Stenhouse adducts. (a) top: Meldrum's acid acceptor; bottom: Barbituric acid acceptor. Reagents and conditions: (i) H_2O and (ii) aniline-derivative, neat, DCM, MeOH or THF. (b) Select properties of three representative secondary aniline-based DASAs highlighting stark differences for subtle changes in chemical structure; N-methyaniline, tetrahydroquinoline, and indoline from left to right.

Aniline of DASA 7			
λ_{max} (nm)	582	599	615
ϕ_{D-A} (°)	38	24	0
pK_a of aniline	4.9	5.2	5.6
% in open form	11%	17%	31%
ε (M^{-1} cm^{-1})	1×10^6	1×10^6	1×10^6

that absorb visible and near-IR light (ranging from 450 to 750 nm) in solvents of varying polarity as well as in polymer matrices. Detailed characterization to elucidate structure−property relationships for these second generation aniline-based donors is also provided. We show that wavelength tunability can be exploited in systems where two different DASAs can be independently switched in both solution and polymer films.

RESULTS AND DISCUSSION

Synthesis. We have developed a two-step procedure from commercially available starting materials for the synthesis of aniline-based DASAs (Figure 2a). First, an activated furan-carbon acid is generated by condensing furfural, an inexpensive (~$2/kg) byproduct from nonedible biomass, with either Meldrum's or barbituric acid. The synthesis is performed in water at either room temperature (barbituric acid) or 70 °C (Meldrum's acid), where the pure product precipitates out of solution as a yellow solid in near quantitative yield.[31] Isolation and purification are accomplished by filtration and subsequent washing with water. Second, the activated furan adduct is mixed with a secondary aniline derivative either neat using 3−5 equiv of the amine or in solution using 1 equiv. Less nucleophilic aniline derivatives, such as N-methylaniline, require neat conditions for optimal yields, whereas more electron-rich/nucleophilic anilines, such as indoline or 5-methoxyindole, can be run in tetrahydrofuarn (THF) or dichloromethane (DCM). Purification is accomplished by trituration with hexanes, diethyl ether, or THF, yielding the desired DASA products as dark lustrous solids.

With efficient access to a range of aniline-based DASAs, it was evident immediately that subtle differences in the aniline donor results in dramatic changes in color and the ability to switch reversibly in a number of solvents. Probing aniline-based DASAs bearing N-methylaniline, tetrahydroquinoline, and indoline donors in detail revealed a number of property trends that could be correlated back to the structure, including peak absorption (λ_{max}), calculated dihedral angle between the donor and acceptor (Φ_{D-A}), negative log of the acid dissociation constant (pK_a) of the donor amine, open/close equilibrium percentage, and molar absorptivity (ε), (Figure 2b; characterization data for all DASAs is provided in Table S1).

Property Studies. The bathochromic shift in absorption of the aniline-based DASAs relative to the alkyl-based DASAs was the first property we sought to evaluate. Meldrum's acid and barbituric acid acceptors were both synthesized and characterized with representative absorption spectra given for the barbituric acid derivatives in Figure 3 (the full barbituric acid and Meldrum's acid derivatives are described in Figures S1 and S2). The same absorption trends are observed for both barbituric and Meldrum's acid-based DASAs, but all wavelengths are bathochromically shifted by approximately 25 nm for the barbituric structures. The peak absorptions for N-methylaniline (8), tetrahydroquinoline (9), and indoline (10) are 582, 599, and 615 nm, respectively (Figures 2b and 3). The wavelength could be extended further by incorporating electron donating groups at the para position of the cyclic anilines, such as methoxy (11) and N,N-dialkyl (12), which led to red-shifts in absorption (λ_{max} = 629 and 669 nm, respectively) compared to that of native indoline (λ_{max} = 615 nm). The most notable structural difference between these derivatives and the alkyl-based DASAs is the presence of an aromatic ring, where homoconjugation may result in a bathochromic absorption shift due to enhanced hybridization of molecular orbitals between the electron-rich donors and acceptor groups, an effect
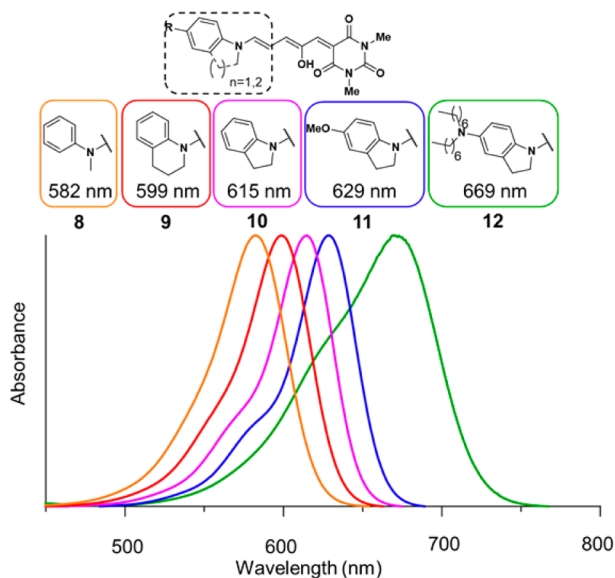
Figure 3. Representative absorption spectra for aniline-based DASAs highlighting the wavelength tunability with barbituric acid derivatives. Measured as 10 μM solutions in DCM.

commonly observed with "push-pull" systems in organic semiconductors.[35,36] Using readily available aniline-based donors, the absorbance maxima of barbituric-based DASAs were tuned from 582 to 669 nm.

In contrast to the cyclic indoline derivatives, acyclic derivatives such as p-methoxy-N-methylaniline do not lead to a significant change in λ_{max} compared to unsubstituted N-methylaniline (Figure 4 and Figure S3). For the difference

	λ_{max} (nm)	Φ_{D-A} (°)	λ_{max} (nm)	Φ_{D-A} (°)
R = H	559	39	589	0
R = OMe	561	42	602	0
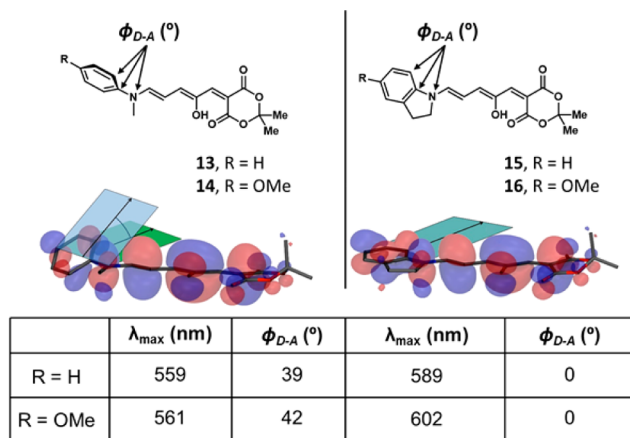
Figure 4. Computational density functional theory modeling of representative aniline DASAs, determining HOMO orbital overlap, energy gap (represented by λ_{max}), and dihedral angle between donor and acceptor (Φ_{D-A}).

between acyclic- and cyclic-substituted N-methylaniline derivatives to be addressed, density functional theory (DFT) calculations at the B3LYP/6-31G(d) level were performed to identify the dihedral angle between the donor and acceptor groups (Φ_{D-A}), and the character of the highest occupied molecular orbitals (HOMOs) overlap (Figures 2b and 4 and Figures S4 and S5). N-Methylaniline (8 and 15) derivatives were found to have a substantial out-of-plane twist ($\Phi_{D-A} \approx 40°$), wheras indoline (10 and 16) derivatives were planar

($\Phi_{D-A} \approx 0°$). As a consequence, indoline derivatives have more HOMO overlap/conjugation, resulting in a narrowing of the energy gap (E_g)/bathochromic shift of ~30 nm relative to the corresponding N-methylaniline derivatives. Even more striking than the difference between the acyclic and cyclic anilines is the effect of a donating group para to the aniline nitrogen. Because the N-methylaniline is out of plane, a donating group, such as p-methoxy, has little impact on the wavelength and only results in a 2 nm bathochromic shift compared to its unsubstituted counterpart. However, in the indoline case, the addition of a p-methoxy group causes a 13 nm redshift. Planarity of the aryl ring in the aniline donor is therefore critical for increasing conjugation and extending the absorption maxima wavelength. Of note, these trends can be predicted using DFT calculations (Figure S6).

The molar absorptivities (ε) for N-methylaniline (8), tetrahydroquinoline (9) and indoline (10) barbituric acid derivatives were determined through a combination of NMR and absorption spectroscopies at equilibrium (Figure S7). The ε values for these derivatives are uniformly high at ~10^6 M^{-1} cm^{-1}. The strong dye character for DASAs highlights their potential for colorimetric sensing applications because the naked eye can identify even minute amounts (<1 mg/mL).

During the molar absorptivity investigations, it was observed that an equimolar solution of p-methoxy-N-methylaniline derivative (14) in dichloromethane (DCM) appeared darker and required more time to switch with visible light than that of the corresponding N-methylaniline derivative (13). Because the intensity of color and rate of switching is a critical property for numerous applications of negative photochromes, we sought to better understand this observation. All aniline-based DASAs are isolated in a nearly all open triene (colored) form via precipitation, as seen with ^{1}H NMR spectroscopy (see Supporting Information (SI)); however, given time to thermally equilibrate in solution, the aniline derivatives partially cyclize to the closed cyclopentenone (transparent) form. This process could be monitored by ^{1}H NMR, and it was determined that the equilibrium position could be approximately correlated to the pK_a of the aniline derivatives (Figures S9−S13). For example, the percent of open colored form in CD_2Cl_2 goes from 2 to 12 to 41% for the p-chloro-N-methyaniline (S1), N-methylaniline (13), and p-methoxy-N-methylaniline (14) derivatives, respectively (determined by ^{1}H NMR). As expected, substitution of aniline derivatives will affect basicity,[37] and the pK_a of the conjugate acid of p-chloro-N-methylaniline, N-methylaniline, and p-methoxy-N-methylaniline increases from 4.0 to 4.9 to 5.9. This relationship between pK_a and percent of open form in DCM also exists for the cyclic aniline derivatives. The respective conjugate acid pK_a values for N-methylaniline, tetrahydroquinoline, and indoline are 4.9, 5.1, and 5.5,[38] and the open percent of the open percent of these derivatives these derivatives at equilibrium in DCM goes from 11 to 19 to 31% (Figure 2b and Figure S10). Notably, by using electron-rich 5-diheptylamino indolines (S3 and 13), the donor shifts the equilibrium to nearly 100% in the open form in DCM. This demonstrates that the equilibrium of these systems can be controlled by the basicity of the donor amine, which can also be used to tune the depth of color. Finally, the equilibrium ratio plays a role in the observed rate of switching with electron-deficient anilines switching from colored-to-colorless the most readily.

Kinetics. For aniline-based DASA compounds, it was also observed that the rate of thermal relaxation varied depending

on the derivative, and as such, we sought to investigate the fundamental kinetic properties of this new photochromic system. The opening and closing rates and activation energies (E_A) of the aniline DASAs were determined by ^{1}H NMR spectroscopy. N-Methylaniline (**8**), tetrahydroquinoline (**9**), and indoline (**10**) barbituric acid-derived DASAs were dissolved in deuterated chlorobenzene in the absence of light and allowed to thermally relax to equilibrium (from triene to triene-cyclopentenone mixtures) at four different temperatures inside the NMR. Integration of protons unique to the open triene and closed cyclopentenone forms were utilized to monitor the rate of closing over time. The data obtained from the NMR experiments was fit to an isomer equilibrium model assuming first order rates of opening and closing. The model used was of the form:

$$[A]_t = \frac{k_{\text{open}} + k_{\text{close}}e^{-(k_{\text{close}}+k_{\text{open}})t}}{k_{\text{close}} + k_{\text{open}}}[A]_0$$

where k_{open}, k_{close}, and A_0 represent the rate of opening, the rate of closing, and the initial concentration, respectively. Interestingly, the rates of equilibration were found to increase from tetrahydroquinoline (**9**) < N-methylaniline (**8**) < indoline (**10**), with indoline being ~3.5 times faster than aniline. In addition, by plotting the rate constants relative to $1/T$, we could use the Arrhenius expression to extract activation energies (E_{open} and E_{close}) (Figure 5b and Table S1). The E_{open} and E_{close} values were similar for the three derivatives, ranging from 60 to 71 kJ/mol (Table S1). This is comparable
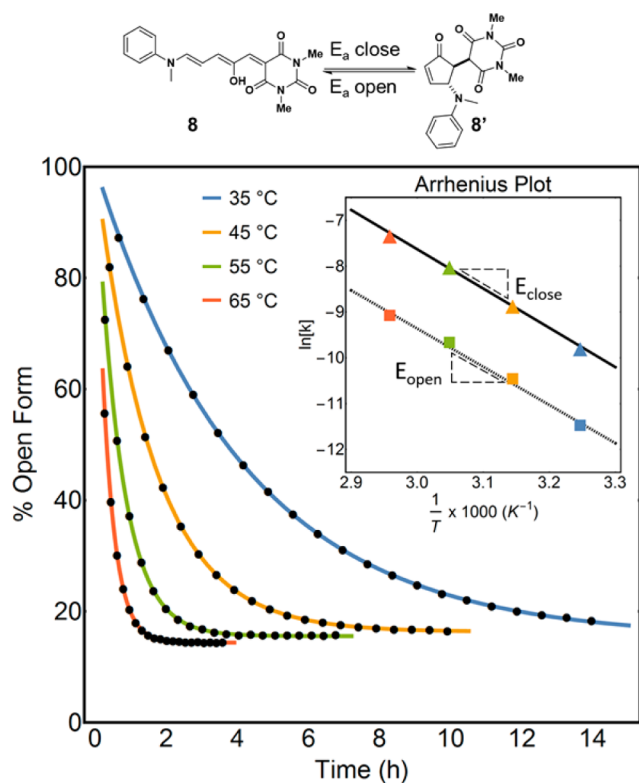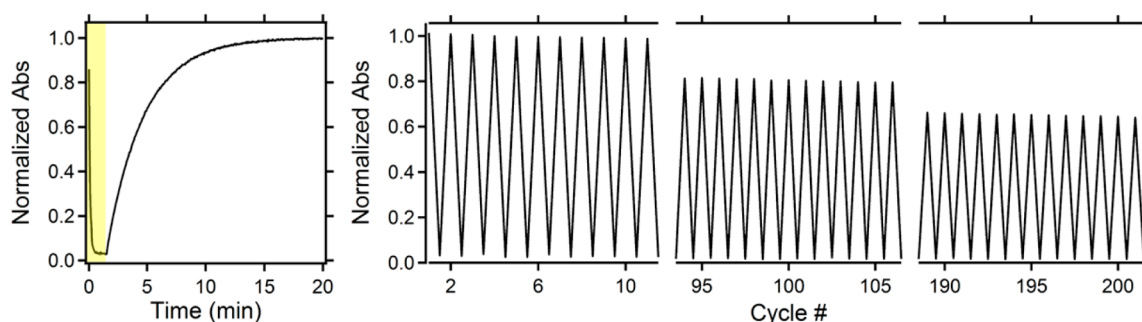
to both experimental and computational results obtained by Feringa[39] and Jacquemin[40] for dialkyl DASAs and lower than the ~90 kJ/mol measured for reported spiropyran-based photoswitches.[18]

Fatigue Resistance. Reversibility and stability are further crucial performance parameters in photochromic systems, in particular for applications that rely on recyclability of the photoswitch (e.g., actuators, sensors, mechanophores, etc.) To test the robustness of these aniline-based DASA derivatives, we performed extensive cycling tests with the p-methoxy indoline barbituric acid derivative **11** given its fast reversible kinetics (Figure 6). Pump−probe absorption spectroscopy with a broadband white light-emitting diode (LED) for excitation and a heated stage for equilibration (50 °C in chlorobenzene, 67% open by ^{1}H NMR) were used for the cycling experiments under ambient atmospheric conditions (i.e., in the presence of oxygen). Figure 6a shows a detailed plot of absorption at λ_{max} (629 nm) during the first cycle, where a snapshot (100 ms exposure time) of the absorption trace was taken every 5 s over the course of 20 min with irradiation for the first 30 s and then off for the remaining time. The following cycles were recorded by taking individual measurements immediately following photoswitching and thermal equilibration (Figure 6b). Similar to the previously reported dialkyl DASAs, minimal degradation was observed after 10 cycles.[32] Extending to 100 cycles then 200 cycles showed slow degradation with 80 and 60% absorbance recovery, respectively, with no observable change to the absorption profile. These in-depth cycling experiments highlight the stability of DASAs in the presence of oxygen and at elevated temperatures, making them good candidates for applications requiring a recyclable color-to-transparent photoswitch that operates under ambient conditions.

Switching Properties. A significant advantage of these second generation aniline-based DASAs is photoswitchability in a variety of solvents. Whereas the previously reported dialkyl DASAs were limited to photoswitching in nonpolar solvents (e.g., toluene, xylenes, etc.), the aniline DASAs are capable of photoswitching in polar solvents such as THF, DCM, ethyl acetate, and acetonitrile as highlighted in Figure 7 for N-methylaniline barbituric acid DASA **8**. In all cases, quantitative photoconversion, evident by the generation of colorless solutions and UV/vis absorption spectroscopy, was observed in a range of solvents with the exception of **12**. In this case, photoswitching was largely limited to less polar solvents such as a toluene/hexanes mixture, presumably due to the increased basicity of the aniline. It is worth noting that one unique aspect of DASA-based photoswitches, compared to azobenzene or acylhydroazones for example, is that photomediated reaction (E−Z alkene isomerization) is coupled with a thermal 4π electrocyclization. As a consequence, this cascade process provides a pathway to leverage a potentially incomplete E−Z alkene isomerization into an efficient photoswitch. However, this also makes the evaluation of photostationary states (PSS) difficult because the Z-isomer can convert to the colorless cyclopentenone adduct.

The ability to efficiently activate the new aniline-derivatives in a variety of solvents is a critical breakthrough that provides the potential for DASA-based photoswitches to be used in numerous applications that require polar matrices (e.g., sensors, mechanophores, etc.).[41] Additionally, alkyl-based DASAs were not readily responsive to visible light when dispersed in a solid polymer matrix irrespective of the polymer tested (e.g., polystyrene, poly(methyl methacrylate), etc.). In direct


Figure 5. Open to closed equilibration kinetics for select N-methylaniline-based barbituric acid DASAs (**8**) determined using ^{1}H NMR spectroscopy in chlorobenzene-d5 at the specified temperatures. (inset) Corresponding Arrhenius plot for determining activation energy.

Figure 6. Pump−probe absorption spectroscopy of *p*-methoxy indoline barbituric acid DASA **11** in chlorobenzene at 50 °C, exciting with a broadband white light-emitting diode. (a) Detailed first cycle showing a rapid photoresponse (<30 s) followed by thermal equilibration over 20 min. (b) Cycling study showing approximately 20% decrease in absorption every 100 cycles.
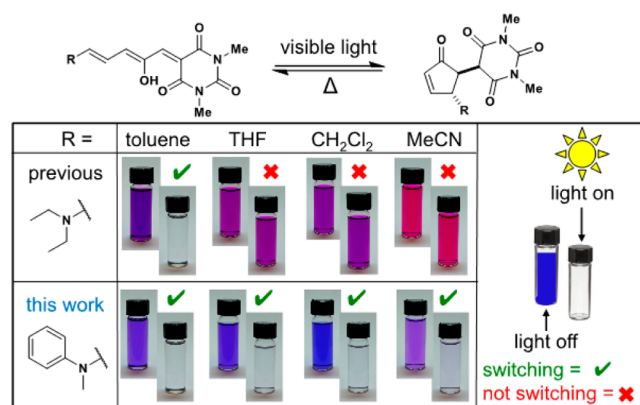
Figure 7. Representative photoswitchability in solvents of varying polarity for alkyl-based DASAs (top) and aniline-based DASAs (bottom). Diethyl- and *N*-methylaniline-barbituric acid DASA was dissolved in the denoted solvent followed by shining a broadband white light source on the sample, taking pictures before and after exposure to light.

contrast, *N*-methylaniline (**8**), tetrahydroquinoline (**9**), and indoline (**10**) barbituric acid DASAs were found to be photoactive as physical blends in polymer matrices (Figure S17). To illustrate this feature, three DASA derivatives were codissolved with poly(methyl methacrylate), poly(ethyl methacrylate), or poly(butyl methacrylate) in DCM (1 wt % DASA relative to polymer), drop-cast onto glass slides, dried at 50 °C, and irradiated with broadband visible light. Significantly, this results in photoswitching in all matrices with the initial color of the equilibrated films having different shades. This is believed to indicate varying ratios of open:closed forms in each matrix, an attribute that we are actively exploring in more detail.

An enabling aspect of the aniline-based DASAs is addressability (the difference in absorption wavelengths between two different isomers or photoswitches), which relies on the inherent tunabilty of the absorption wavelength. This feature is critical for independently controlling two different photoswitches and holds great potential for various applications.[42] Accordingly, we sought to demonstrate the selective switching of two different DASAs in solution (Figure 8).[43] DASA (**13**) bearing an *N*-methylaniline donor and Meldrum's acid acceptor group (λ_{max}, 560 nm in PhMe) and DASA (**11**) bearing a *p*-methoxy indoline donor and barbituric acid acceptor group (λ_{max}, 623 nm in PhMe) were chosen based on their minimal absorption overlap (Figure 8).[44] First, a long-pass 650 nm filter (red light) was used to selectively switch **11** at room temperature, converting the initially violet solution to
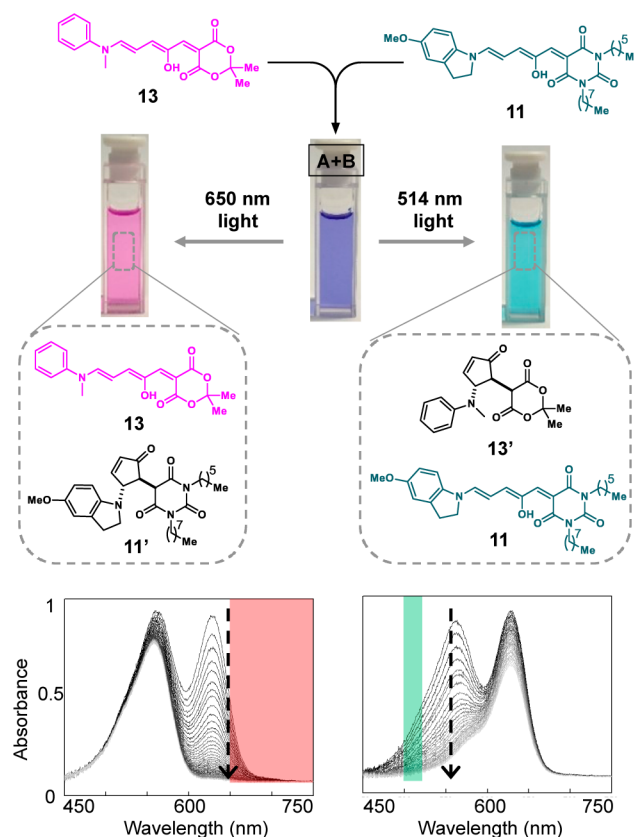

Figure 8. Selective photoswitching of two mixed DASAs, *N*-methylaniline Meldrum's acid **13** and indoline barbituric acid **11** using filtered broadband white LED. Compounds **11** and **13** were mixed in toluene followed by photoswitching through a 514 nm bandpass filter to cyclize **13** or a 650 nm long-pass filter to cyclize **11**.

pink (color of **13**). Of note, the minor decrease at 560 nm during the course of >650 nm irradiation corresponds to photoswitching of **11** (not **13**) due to partial absorption overlap of a shoulder at 560 nm. This was confirmed by running control experiments where red light irradiation of a solution containing only **13** did not lead to photoswitching (Figure S18). For the alternative case, a 514 nm bandpass filter (green light) was used to selectively switch **13** with minimal switching of **11** (Figure S21). As a result, the initial violet solution was converted to turquoise (color of **11**). Alternatively, by using a broad spectrum white LED light source, both DASAs switched to their colorless cyclized form at the same time.

Encouraged by these results, the selective switching methodology was also investigated for the same pairwise combination of DASA derivatives dispersed in a solid matrix of poly(methyl methacrylate) (PMMA). The films were prepared by drop-casting a DCM solution containing 100 mg/mL PMMA and ~1 mg/mL of **11** and **13** onto a glass slide (Scheme 1).

Scheme 1. Selective Photoswitching of Two Mixed DASAs, *N*-Methylaniline Meldrum's Acid 13, and Indoline Barbituric Acid 11 Suspended in Drop-Cast Films Containing ~1 wt % DASA in PMMA Using Filtered Broadband White LED
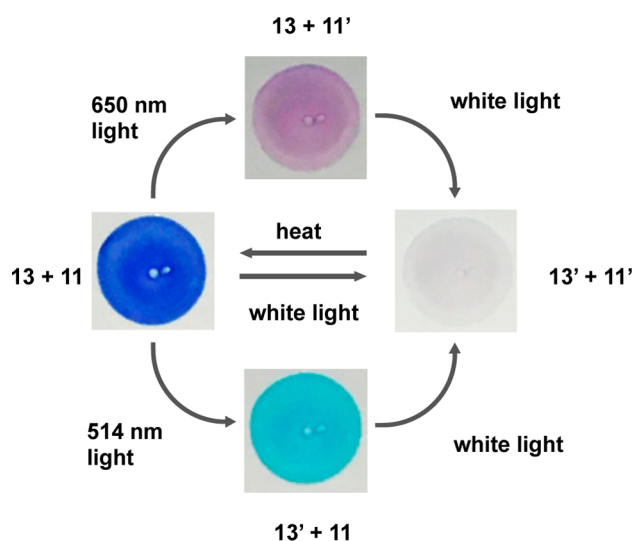
Irradiation of the DASA blend in PMMA with a 650 nm LED again resulted in a distinct color change from purple to pink due to the selective photoswitching of **11**. Alternatively, **13** could be selectively switched by irradiating with a 450 nm LED to give a turquoise film. Finally, broad-spectrum white light led to the cyclization of both derivatives, leaving a transparent film, and heating the sample at 50 °C for 2 min reverted the sample back to its original colored state. This clearly demonstrates for the first time the ability to selectively and reversibly switch mixtures of DASA derivatives in both solution and the solid state.

In summary, a second generation aniline-based donor–acceptor Stenhouse adduct was developed and characterized. The new photochromic platform is highly tunable, providing a wide photoresponsive region from 500–650 nm that is not restricted to solution-state or nonpolar matrices for reversible switchability. Through careful choice of the donor moiety, the wavelength and solvent switching properties can be precisely controlled. This combined with computational modeling and equilibrium kinetics provide valuable guidelines for the development of future DASA systems. Finally, selective switching in both solutions and polymer-matrices highlights the significant potential of inverse DASA photoswitches in materials applications.

ASSOCIATED CONTENT

S **Supporting Information**

The Supporting Information is available free of charge on the ACS Publications website at DOI: 10.1021/jacs.6b07434.

Experimental procedures and characterization data for all compounds (PDF)

AUTHOR INFORMATION

Corresponding Author

*javier@chem.ucsb.edu

Notes

The authors declare the following competing financial interest(s): A patent has been filed on the photochromic materials.

REFERENCES

(1) Szymanski, W.; Beierle, J. M.; Kistemaker, H. A. V; Velema, W. A.; Feringa, B. L. *Chem. Rev.* **2013**, *113*, 6114.
(2) Kawata, S.; Kawata, Y. *Chem. Rev.* **2000**, *100*, 1777.
(3) Russew, M. M.; Hecht, S. *Adv. Mater.* **2010**, *22*, 3348.
(4) Rosario, R.; Gust, D.; Hayes, M.; Jahnke, F.; Springer, J.; Garcia, A. A. *Langmuir* **2002**, *18*, 8062.
(5) Schöller, K.; Küpfer, S.; Baumann, L.; Hoyer, P. M.; De Courten, D.; Rossi, R. M.; Vetushka, A.; Wolf, M.; Bruns, N.; Scherer, L. J. *Adv. Funct. Mater.* **2014**, *24*, 5194.
(6) Shiraishi, Y.; Shirakawa, E.; Tanaka, K.; Sakamoto, H.; Ichikawa, S.; Hirai, T. *ACS Appl. Mater. Interfaces* **2014**, *6*, 7554.
(7) Kundu, P. K.; Samanta, D.; Leizrowice, R.; Margulis, B.; Zhao, H.; Börner, M.; Udayabhaskararao, T.; Manna, D.; Klajn, R. *Nat. Chem.* **2015**, *7*, 646.
(8) Dong, M.; Babalhavaeji, A.; Samanta, S.; Beharry, A. A.; Woolley, G. A. *Acc. Chem. Res.* **2015**, *48*, 2662.
(9) Beharry, A. A.; Woolley, G. A. *Chem. Soc. Rev.* **2011**, *40*, 4422.
(10) Velema, W. A.; Szymanski, W.; Feringa, B. L. *J. Am. Chem. Soc.* **2014**, *136*, 2178.
(11) Beharry, A. A.; Sadovski, O.; Woolley, G. A. *J. Am. Chem. Soc.* **2011**, *133*, 19684.
(12) Samanta, S.; Beharry, A. A.; Sadovski, O.; Mccormick, T. M.; Babalhavaeji, A.; Tropepe, V.; Woolley, G. A. *J. Am. Chem. Soc.* **2013**, *135*, 9777.
(13) Barrett, C. J.; Mamiya, J.; Yager, K. G.; Ikeda, T. *Soft Matter* **2007**, *3*, 1249.
(14) Li, J.; Nagamani, C.; Moore, J. S. *Acc. Chem. Res.* **2015**, *48*, 2181.
(15) Bandara, H. M. D.; Burdette, S. C. *Chem. Soc. Rev.* **2012**, *41*, 1809.
(16) Irie, M.; Fukaminato, T.; Matsuda, K.; Kobatake, S. *Chem. Rev.* **2014**, *114*, 12174.
(17) Broman, S. L.; Petersen, M. Å.; Tortzen, C. G.; Kadziola, A.; Kilså, K.; Nielsen, M. B. *J. Am. Chem. Soc.* **2010**, *132*, 9165.
(18) Minkin, V. I. *Chem. Rev.* **2004**, *104*, 2751.
(19) Yamaguchi, T.; Kobayashi, Y.; Abe, J. *J. Am. Chem. Soc.* **2016**, *138*, 906.
(20) Tanaka, M.; Ikeda, T.; Xu, Q.; Ando, H.; Shibutani, Y.; Nakamura, M.; Sakamoto, H.; Yajima, S.; Kimura, K. *J. Org. Chem.* **2002**, *67*, 2223.
(21) Ayub, K.; Mitchell, R. H. *J. Org. Chem.* **2014**, *79*, 664.
(22) Minami, M.; Taguchi, N. *Chem. Lett.* **1996**, *25*, 429.
(23) Hatano, S.; Horino, T.; Tokita, A.; Oshima, T.; Abe, J. *J. Am. Chem. Soc.* **2013**, *135*, 3164.
(24) Yang, Y.; Hughes, R. P.; Aprahamian, I. *J. Am. Chem. Soc.* **2014**, *136*, 13190.

(25) Yang, Y.; Hughes, R. P.; Aprahamian, I. *J. Am. Chem. Soc.* **2012**, *134*, 15221.

(26) Bléger, D.; Schwarz, J.; Brouwer, A. M.; Hecht, S. *J. Am. Chem. Soc.* **2012**, *134*, 20597.

(27) Siewertsen, R.; Neumann, H.; Buchheim-Stehn, B.; Herges, R.; Näther, C.; Renth, F.; Temps, F. *J. Am. Chem. Soc.* **2009**, *131*, 15594.

(28) Mason, B. P.; Whittaker, M.; Hemmer, J.; Arora, S.; Harper, A.; Alnemrat, S.; Mceachen, A.; Helmy, S.; Read de Alaniz, J.; Hooper, J. P. *Appl. Phys. Lett.* **2016**, *108*, 041906.

(29) Li, X.; Li, J.; Wang, Y.; Matsuura, T.; Meng, J. *J. Photochem. Photobiol., A* **2004**, *161*, 201.

(30) Radu, A.; Byrne, R.; Alhashimy, N.; Fusaro, M.; Scarmagnani, S.; Diamond, D. *J. Photochem. Photobiol., A* **2009**, *206*, 109.

(31) Helmy, S.; Oh, S.; Leibfarth, F. A.; Hawker, C. J.; Read de Alaniz, J. *J. Org. Chem.* **2014**, *79*, 11316.

(32) Helmy, S.; Leibfarth, F. A.; Oh, S.; Poelma, J. E.; Hawker, C. J.; Read de Alaniz, J. *J. Am. Chem. Soc.* **2014**, *136*, 8169.

(33) Singh, S.; Friedel, K.; Himmerlich, M.; Lei, Y.; Schlingloff, G.; Schober, A. *ACS Macro Lett.* **2015**, *4*, 1273.

(34) Balamurugan, A.; Lee, H. *Macromolecules* **2016**, *49*, 2568.

(35) Cheng, Y.-J.; Yang, S.-H.; Hsu, C.-S. *Chem. Rev.* **2009**, *109*, 5868.

(36) Li, Y. *Acc. Chem. Res.* **2012**, *45*, 723.

(37) Kanzian, T.; Nigst, T. A.; Maier, A.; Pichl, S.; Mayr, H. *Eur. J. Org. Chem.* **2009**, *36*, 6379.

(38) Yang, D.; Zuccarello, G.; Mattes, B. R. *Macromolecules* **2002**, *35*, 5304.

(39) Lerch, M. M.; Wezenberg, S. J.; Szymanski, W.; Feringa, B. L. *J. Am. Chem. Soc.* **2016**, *138*, 6344.

(40) Laurent, A.; Medved, M.; Jacquemin, D. *ChemPhysChem* **2016**, *17*, 1846.

(41) Of note, the ability to photoswitch in a given solvent depends on the basicity of the amine. The N-methyl aniline DASAs readily switched in a variety of solvents, whereas the 5-diheptylamino-indole derivatives photoswitched only in nonpolar solvents such as toluene or hexanes.

(42) Hansen, M. J.; Velema, W. A.; Lerch, M. M.; Szymanski, W.; Feringa, B. L. *Chem. Soc. Rev.* **2015**, *44*, 3358.

(43) Lerch, M. M.; Hanson, M. J.; Velema, W. A.; Szmanski, W.; Feringa, B. L. *Nat. Commun.* **2016**, *7*, 12504.

(44) The absorption for each DASA at equilibrium was normalized and pump−probe measurements with a filtered white LED was used to monitor changes in absorption over time.